

Identification of post-pyrite phase transitions in SiO₂ by a genetic algorithmShunqing Wu,^{1,2} Koichiro Umemoto,³ Min Ji,¹ Cai-Zhuang Wang,¹ Kai-Ming Ho,¹ and Renata M. Wentzcovitch⁴¹*Ames Laboratory, US DOE and Department of Physics and Astronomy, Iowa State University, Ames, Iowa 50011, USA*²*Department of Physics, Xiamen University, Xiamen 361005, China*³*Department of Geology and Geophysics, University of Minnesota, Minneapolis, Minnesota 55455, USA*⁴*Minnesota Supercomputing Institute and Department of Chemical Engineering and Materials Science,**University of Minnesota, Minneapolis, Minnesota 55455, USA*

(Received 31 March 2011; published 16 May 2011)

Using a first-principles genetic algorithm we predict an Fe₂P phase is the first post-pyrite phase of SiO₂ at low temperatures. This contrasts with a recently predicted cotunnite phase. Static enthalpy differences between these two phases are small near the transition pressure (0.69 TPa). While quasiharmonic free energy calculations predict an Fe₂P→cotunnite-type transition with increasing temperature, another phase, NbCoB type, is identified as being structurally and energetically intermediate between Fe₂P and cotunnite phases. This structure suggests a possible temperature-induced gradual transformation between Fe₂P and cotunnite phases. This finding would change our understanding of how planet-forming silicates, for example, MgSiO₃ post-perovskite and its solid solutions, dissociate into elementary oxides at thermodynamic conditions expected in the interior of solar giants and exoplanets.

DOI: [10.1103/PhysRevB.83.184102](https://doi.org/10.1103/PhysRevB.83.184102)

PACS number(s): 64.70.K-, 61.50.Ks, 91.60.Gf

I. INTRODUCTION

MgSiO₃ is a major constituent of Earth's mantle. The discovery of the post-perovskite (PPV) transition of MgSiO₃ near Earth's core-mantle boundary conditions¹⁻³ reminded us that minerals can have truly unexpected high-pressure behavior. This finding naturally introduced a new question: what is the next high-pressure polymorph of MgSiO₃? The answer is fundamental for modeling the interiors of recently discovered exoplanets, particularly the terrestrial type,^{4,5} and the cores of the solar giants, where pressures and temperatures can reach 4 TPa and 21 000 K.⁶ In 2006 the dissociation of MgSiO₃ PPV into CsCl-type MgO and cotunnite-type SiO₂ was predicted at 1.1 TPa.⁷ This prediction was based on the assumption of a sequence of pressure-induced transitions in SiO₂: rutile → CaCl₂ → α-PbO₂ → pyrite → cotunnite phases. Experimentally, only phases up to pyrite-type SiO₂ have been observed to date.⁸ This sequence of transitions seemed very reasonable because (i) MgF₂, a low-pressure analog of SiO₂, undergoes the same sequence of pressure-induced transitions from rutile up to pyrite and then transitions to the cotunnite phase⁹ preceded by phase X in a very narrow pressure range¹⁰ and (ii) the cotunnite phase has cation coordination number (CN) higher (9) than that of the pyrite phase (6). Nevertheless, it is not guaranteed at all that the cotunnite phase is the real post-pyrite phase of SiO₂. The predicted transition pressure to the cotunnite phase (~0.69 TPa)^{7,11} is still too high to be observed in static compression experiments. Prediction of high-pressure phases in the multi-Mbar regime is a difficult problem and behavior of low-pressure analogs is often invoked. Comparison of enthalpies and/or Gibbs free energies of potential structures is the method frequently used (Refs. 11 and 12 for postpyrite SiO₂) to predict phases at ultrahigh pressures. However, these strategies do not guarantee that the true stable structure is identified. Structural search using genetic algorithms (GA) are much more likely to catch truly stable phases and this method has been proven to work very efficiently.¹³⁻¹⁵ Here we show

that a first-principles GA search predicts the Fe₂P phase as the first post-pyrite phase of SiO₂. The cotunnite phase has very competitive enthalpy but definitely higher than that of the Fe₂P phase beyond the stability field of the pyrite structure. However, the cotunnite phase is stable at high temperatures according to quasiharmonic (QHA) free-energy calculations.¹⁶ These two structures are very closely related, and the existence of another competitive and structurally intermediate phase, the NbCoB type, suggests a gradual crossover between them. We also discuss the effect of these new phase transitions on the dissociation of MgSiO₃ PPV.

II. COMPUTATIONAL METHOD

First-principles GA structural searches were performed at 0.5 and 2 TPa. The details of our GA algorithm were described elsewhere.¹⁵ The number of structures in the GA pool was 32 or 64. The candidate structure pool was initially generated from experimentally known and randomly generated structures. We considered primitive cells with 1–8 SiO₂ formula units (FUs). We used the local density approximation (LDA).^{17,18} Two sets of silicon and oxygen pseudopotentials were generated by Vanderbilt's method.¹⁹ For the GA searches we used pseudopotentials generated using the following electronic configurations: 3s²3p¹3d⁰ and 2s²2p⁴ with cutoff radii of 1.6 and 1.4 a.u. for silicon and oxygen, respectively. They required a cutoff energy of 40 Ry. Brillouin-zone integration was performed using the Monkhorst-Pack sampling scheme²⁰ over **k**-point meshes of spacing 2π × 0.05 Å⁻¹. In the structure relaxation steps, constant-pressure variable-cell-shape molecular dynamics^{21,22} was used. Candidate structures obtained with the GA were refined and their static enthalpies and QHA free energies were calculated using harder pseudopotentials, more suitable for the extreme pressures addressed here.⁷ The valence electronic configurations of these harder pseudopotentials were 2s²2p⁶3s¹3p⁰ and 2s²2p⁴3d⁰ with cutoff radii of 1.2 and 1.0 a.u. for silicon and oxygen, respectively.

Their cutoff energy was 400 Ry. We used density-functional perturbation theory to compute dynamical matrices at $2 \times 2 \times 2$ \mathbf{q} -point mesh for all phases.^{23,24} Phonon frequencies were then calculated by interpolation onto \mathbf{q} -point meshes fine enough to achieve convergence of QHA free energy within 1 mRy/FU. All first-principles calculations were performed using the Quantum-ESPRESSO software distribution,²⁵ which has been interfaced with the GA scheme in a fully paralleled manner.

III. RESULTS AND DISCUSSION

The present GA scheme is quite efficient in this system at high pressure. It takes approximately 10 generations at most to reach ground-state configurations for inspected cases. For instance, at 0.5 TPa the GA search using 4-FU SiO_2 produces a pyrite ground state in just a few generations (as shown in Fig. 1). At 2 TPa, for 4-FU SiO_2 , the cotunnite structure is predicted to be the ground state. For 3-FU SiO_2 at both 0.5 and 2 TPa, the Fe_2P structure is rapidly predicted. For 6-FU and 8-FU SiO_2 , Fe_2P and cotunnite structures are predicted, respectively. These results indicate that Fe_2P and cotunnite phases are indeed good candidates for post-pyrite phases of SiO_2 .

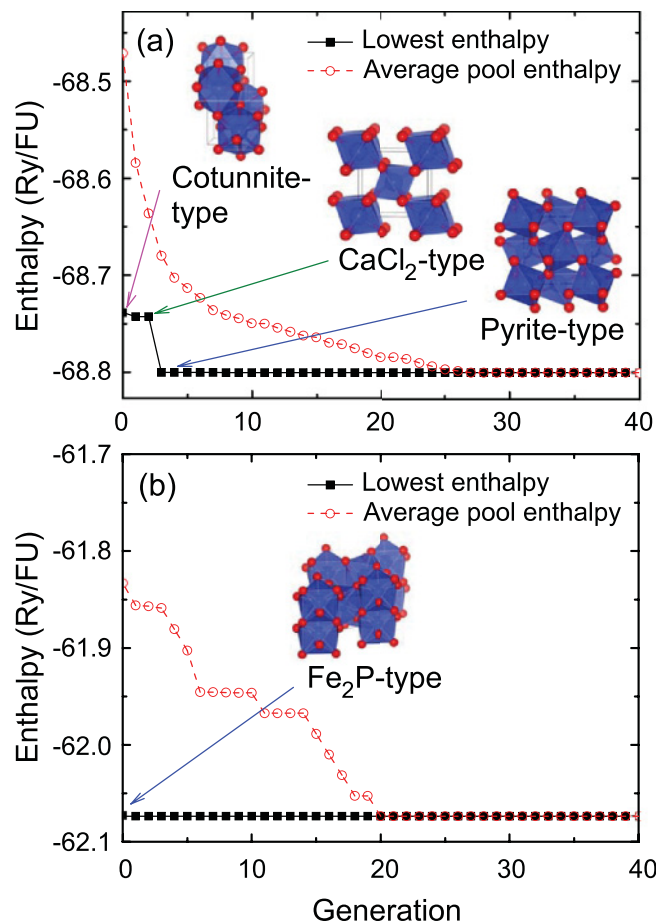


FIG. 1. (Color online) The histories of the lowest energy (enthalpy) and the average pool energy (enthalpy) of (a) 4-FU at 0.5 TPa and (b) 3-FU SiO_2 at 2.0 TPa by generation.

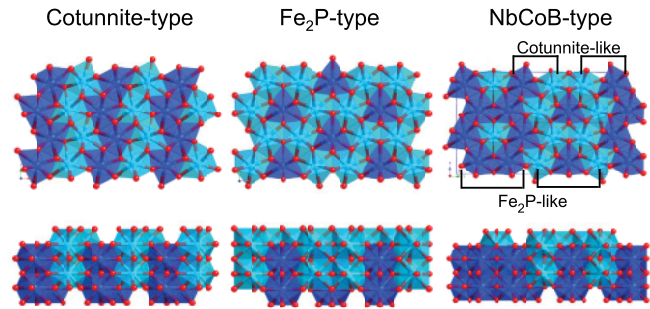


FIG. 2. (Color online) Crystal structures of Fe_2P -, cotunnite- and NbCoB-type phases. Blue and light blue spheres denote silicon atoms at different heights. Red small spheres denote oxygen atoms.

Fe_2P and cotunnite structures (Fig. 2) are closely related.^{26,27} Both have tricapped triangular prisms as structural units with silicon coordination number (CN) equal to 9 ($= 6 + 3$). The lower-pressure phases of SiO_2 (rutile, CaCl_2 , $\alpha\text{-PbO}_2$, and pyrite) consist of Si octahedra. In the $\alpha\text{-PbO}_2$ structure, shifts of silicons from the octahedral center to the middle of an octahedral face give rise to tricapped triangular prisms.²⁷ If all silicons shift in the same direction, the $\alpha\text{-PbO}_2$ structure transforms into the cotunnite structure. If half of silicons shift in the opposite direction, the $\alpha\text{-PbO}_2$ structure changes into the Fe_2P structure. Several other structures with tricapped triangular prisms can be produced by different shifting patterns. Among them, the NbCoB structure, whose unit cell consists of 10 FUs,²⁸ is worthy of note because it is intermediate between Fe_2P and cotunnite structures. In this structure Fe_2P and cotunnite structures appear in an alternating pattern (Fig. 2). Therefore the NbCoB phase is also a potential post-pyrite phase. Calculated structural parameters of these three potential post-pyrite phases of SiO_2 are given in Table I.

Several other phases appeared in GA pools. Among them, the Li_2ZrF_6 structure²⁹ is also worthy of note. This phase consists of silicon octahedra and is closely related to the $\alpha\text{-PbO}_2$ structure,²⁷ in the same way as Fe_2P and cotunnite structures are related. Fe_2P and cotunnite structures with tricapped triangular prisms are structural counterparts of Li_2ZrF_6 and $\alpha\text{-PbO}_2$ structures with octahedra. Fe_2P -type SiO_2 can be obtained from Li_2ZrF_6 type by shifting all silicons in the same direction from octahedral centers to octahedral faces. Similarly to the NbCoB structure, there might be an intermediate phase between $\alpha\text{-PbO}_2$ and Li_2ZrF_6 as well. At 2 TPa, most phases in GA pools, including the baddeleyite phase, are found to consist of capped triangular prisms. Enthalpy calculations with harder pseudopotentials confirm that these phases are metastable over the entire pressure range investigated here; Li_2ZrF_6 -type SiO_2 has higher enthalpy than $\alpha\text{-PbO}_2$ type at all pressures.

Figure 3 shows relative enthalpies of several phases of SiO_2 . The PBE-type generalized gradient approximation³⁰ give rise to the same results as LDA essentially. Calculated transition pressures by PBE is higher by just ~ 10 GPa, as usually expected.³¹ Static calculations show that pyrite-type SiO_2 transforms to Fe_2P type at 0.69 TPa, being consistent with Ref. 12. This transition pressure is almost identical to the metastable transition pressure between pyrite-type and

TABLE I. Structural parameters of Fe₂P-, cotunnite-, and NbCoB-type SiO₂ at 0.8 TPa. Bulk modulus (*B*) and its pressure derivative (*B'*) at 0.8 TPa were obtained by the third-order Birch-Murnaghan equation of states.

Fe ₂ P-type SiO ₂		
Space group		<i>P</i> $\bar{6}2m$
(<i>a, c</i>)		(4.120 Å, 2.222 Å)
Si ₁	2 <i>c</i>	(1/3, 2/3, 0)
Si ₂	1 <i>b</i>	(0, 0, 1/2)
O ₁	3 <i>f</i>	(0.2567, 0, 0)
O ₂	3 <i>g</i>	(0.5903, 0, 1/2)
(<i>B, B'</i>)		(2.76 TPa, 2.71)
Cotunnite-type SiO ₂		
Space group		<i>Pnma</i>
(<i>a, b, c</i>)		(4.108 Å, 2.191 Å, 4.853 Å)
Si	4 <i>c</i>	(0.2335, 1/4, 0.1387)
O ₁	4 <i>c</i>	(0.3472, 1/4, 0.4347)
O ₂	4 <i>c</i>	(0.9845, 1/4, 0.6670)
(<i>B, B'</i>)		(2.75 TPa, 2.71)
NbCoB-type SiO ₂		
Space group		<i>Pmmn</i>
(<i>a, b, c</i>)		(2.218 Å, 12.010 Å, 4.094 Å)
Si ₁	4 <i>e</i>	(1/4, 0.4470, 0.7612)
Si ₂	4 <i>e</i>	(1/4, 0.3500, 0.2629)
Si ₃	2 <i>b</i>	(1/4, 3/4, 0.2375)
O ₁	4 <i>e</i>	(1/4, 0.5675, 0.5202)
O ₂	4 <i>e</i>	(1/4, 0.6287, 0.025)
O ₃	2 <i>b</i>	(1/4, 3/4, 0.6454)
O ₄	4 <i>e</i>	(1/4, 0.4722, 0.1542)
O ₅	4 <i>e</i>	(1/4, 0.3270, 0.6330)
O ₆	2 <i>a</i>	(1/4, 1/4, 0.0198)
(<i>B, B'</i>)		(2.75 TPa, 2.71)

cotunnite-type SiO₂. Although cotunnite and NbCoB phases are metastable over all pressures in static calculations, their enthalpies are very competitive. Below 0.64 TPa, the cotunnite phase has lower enthalpy than Fe₂P. Above 0.78 TPa, the NbCoB phase has intermediate enthalpy between those of Fe₂P and cotunnite phases. At 1 TPa, enthalpy differences between

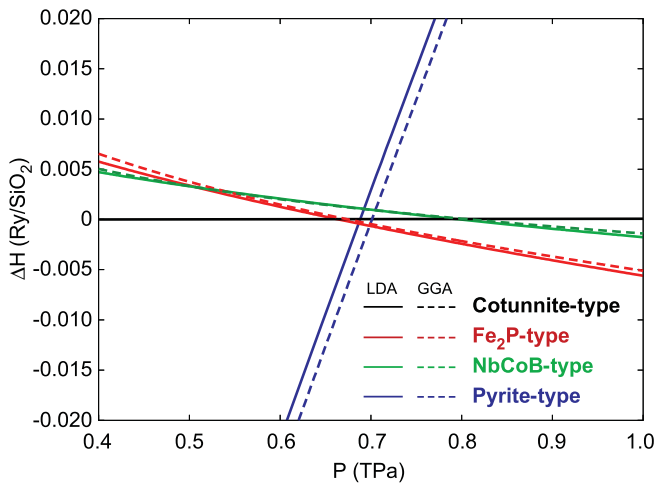


FIG. 3. (Color online) Enthalpies of pyrite-, Fe₂P-, and NbCoB-type SiO₂ with respect to cotunnite-type SiO₂.

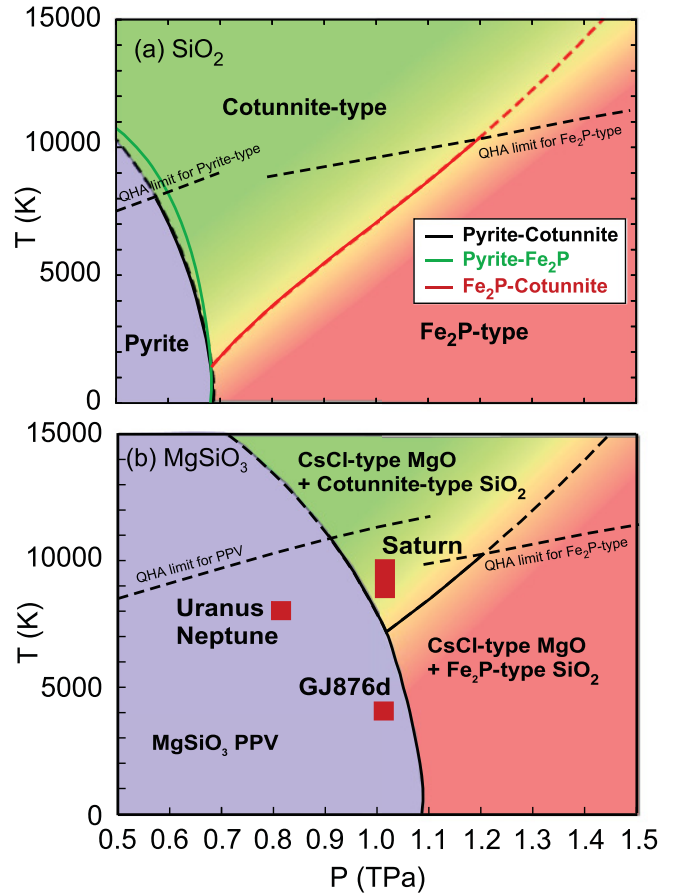


FIG. 4. (Color online) Pressure-temperature phase diagram of (a) SiO₂ and (b) dissociation of MgSiO₃ PPV into MgO and SiO₂. Free energy of MgSiO₃ PPV published in Ref. 7 is used. The transformation between Fe₂P- and cotunnite-type SiO₂ is expected to be gradual (see the text). Red areas denote estimated pressure-temperature conditions at core-envelope boundaries in the solar giants⁶ and in the GJ876d.³⁴ Dashed lines indicate the limit of validity of the QHA.

cotunnite and Fe₂P and between NbCoB and Fe₂P phases are just 0.006 and 0.004 Ry/FU. At 2 TPa, these differences increase to 0.017 and 0.01 Ry/FU (at most ~3000 K). Phonon calculations show that all three phases are dynamically stable beyond ~0.4 TPa.

Figure 4(a) shows the phase diagram of SiO₂ predicted by the QHA. Post-pyrite transitions to Fe₂P and cotunnite phases have negative Clapeyron slopes. This results from the increase in CNs and bond lengths in Fe₂P and cotunnite phases, which increases density of states of low-frequency vibrations and vibrational entropies across these post-pyrite transitions.³² In contrast, the phase boundary between Fe₂P and cotunnite phases has a normal positive Clapeyron slope. Below (above) ~1500 K, pyrite-type SiO₂ should transform to a Fe₂P-type (cotunnite-type) SiO₂. In contrast, the NbCoB phase does not have a stability field. However, entropic stabilization of disordered structural motifs intermediate between Fe₂P and cotunnite is very likely at high temperatures. Therefore the Fe₂P to cotunnite transition might not be sharp but a rather gradual transformation. Actually, the possibility that a fully disordered, mixed, or even dynamically disordered phase is

stable at high temperatures cannot be discarded. However, the cotunnite phase is very stable without phonon instabilities in the pressure and temperature range of the phase diagram we presented, suggesting a crossover.

The presence of the Fe_2P phase introduces an additional phase boundary in the dissociation phase diagram of MgSiO_3 PPV as shown in Fig. 4(b). In the icy giants, Uranus and Neptune, the dissociation into MgO and SiO_2 should not occur. In the gas giants, Saturn and Jupiter, the dissociation into CsCl-type MgO and cotunnite-type SiO_2 occurs first. At higher pressures, depending on the internal temperature profiles in these planets, cotunnite-type SiO_2 might transform to Fe_2P type. In GJ876d, a terrestrial exoplanet³³ with ~ 7.5 Earth masses ($7.5M_\oplus$), conditions estimated at the core-mantle boundary³⁴ are close to the dissociation phase boundary.

Finally, the predicted structural crossover between Fe_2P and cotunnite phases should be fundamental to understanding the high-pressure and high-temperature behavior of AX_2 -type compounds. Although pressures for the predicted phenomenon in SiO_2 are challenging to experiments, low-pressure analogs could be investigated to validate our predictions. MgF_2 is particularly suitable because it has a very similar sequence of phase transitions to SiO_2 . In combination with NaF it

forms NaMgF_3 perovskite, that has the same sequence of predicted phase transitions as MgSiO_3 perovskite,^{7,35} including dissociation into elementary fluorides/oxides. There are still unresolved questions in the experimental high-pressure behavior of NaMgF_3 and MgF_2 .^{10,36} The structural crossover between Fe_2P and cotunnite phases might be part of the answer.

ACKNOWLEDGMENTS

Work at Ames Laboratory was supported by the US Department of Energy, Basic Energy Sciences, Division of Materials Science and Engineering, under Contract No. DE-AC02-07CH11358, including a grant of computer time at the National Energy Research Supercomputing Center (NERSC) in Berkeley, CA. K.U. and R.M.W.'s work were supported by NSF Grants No. EAR-0757903, No. EAR-0810272, No. EAR-1047629, and No. ATM-0426757 (VLab). Computations at the University of Minnesota were performed at the Minnesota Supercomputing Institute and at the Laboratory for Computational Science and Engineering. During the review process, a paper reporting the Fe_2P -type phase of SiO_2 by Tsuchiya and Tsuchiya was published.³⁷

-
- ¹M. Murakami, K. Hirose, K. Kawamura, N. Sata, and Y. Ohishi, *Science* **304**, 855 (2004).
- ²A. R. Oganov and S. Ono, *Nature (London)* **430**, 445 (2004).
- ³T. Tsuchiya, J. Tsuchiya, K. Umemoto, and R. M. Wentzcovitch, *Earth Planet. Sci. Lett.* **224**, 241 (2004).
- ⁴A. P. van den Berg, D. A. Yuen, G. L. Beebe, and M. D. Christiansen, *Phys. Earth Planet. Inter.* **178**, 136 (2010).
- ⁵D. D. Sasselov and D. Valencia, *Sci. Am.* **303**(2), 38 (2010).
- ⁶T. Guillot, *Phys. Today* **57**(4), 63 (2004).
- ⁷K. Umemoto, R. M. Wentzcovitch, and P. B. Allen, *Science* **311**, 983 (2006).
- ⁸Y. Kuwayama, K. Hirose, N. Sata, and Y. Ohishi, *Science* **309**, 923 (2005).
- ⁹J. Haines, J. M. Leger, F. Gorelli, D. D. Klug, J. S. Tse, and Z. Q. Li, *Phys. Rev. B* **64**, 134110 (2001).
- ¹⁰B. Grocholski, S.-H. Shim, and V. B. Prakapenka, *Geophys. Res. Lett.* **37**, L14204 (2010).
- ¹¹A. R. Oganov, M. J. Gillan, and G. D. Price, *Phys. Rev. B* **71**, 064104 (2005).
- ¹²T. Tsuchiya, J. Tsuchiya, A. Metsue, and T. Ishikawa, *Acta Mineralogica-Petrographica* **6**, 810 (2010).
- ¹³A. R. Oganov and C. W. Glass, *J. Chem. Phys.* **124**, 244704 (2006).
- ¹⁴G. Trimarchi and A. Zunger, *J. Phys. Condens. Matter*, **20**, 295212 (2008).
- ¹⁵M. Ji, C.-Z. Wang, and K.-M. Ho, *Phys. Chem. Chem. Phys.* **12**, 11617 (2010).
- ¹⁶D. Wallace, *Thermodynamics of Crystals* (Wiley, New York, 1972).
- ¹⁷D. M. Ceperley and B. J. Alder, *Phys. Rev. Lett.* **45**, 566 (1980).
- ¹⁸J. P. Perdew and A. Zunger, *Phys. Rev. B* **23**, 5048 (1981).
- ¹⁹D. Vanderbilt, *Phys. Rev. B* **41**, R7892 (1990).
- ²⁰H. J. Monkhorst and J. D. Pack, *Phys. Rev. B* **13**, 5188 (1976).
- ²¹R. M. Wentzcovitch, *Phys. Rev. B* **44**, 2358 (1991).
- ²²R. M. Wentzcovitch, J. L. Martins, and G. D. Price, *Phys. Rev. Lett.* **70**, 3947 (1993).
- ²³S. Baroni, S. de Gironcoli, A. Dal Corso, and P. Giannozzi, *Rev. Mod. Phys.* **73**, 515 (2001).
- ²⁴P. Giannozzi, S. de Gironcoli, P. Pavone, and S. Baroni, *Phys. Rev. B* **43**, 7231 (1991).
- ²⁵P. Giannozzi *et al.*, *J. Phys. Condens. Matter* **21**, 395502 (2009).
- ²⁶P. Dera, B. Lavina, L. A. Borkowski, V. B. Prakapenka, S. R. Sutton, M. L. Rivers, R. T. Downs, N. Z. Boctor, and C. T. Prewitt, *Geophys. Res. Lett.* **35**, L10301 (2008).
- ²⁷B. G. Hyde and S. Andersson, *Inorganic Crystal Structures* (Wiley, New York, 1989).
- ²⁸P. I. Kryp'yakevich, Y. B. Kuz'ma, Y. V. Voroshilov, C. B. Shoemaker, and D. P. Shoemaker, *Acta Crystallogr. Sect. B* **27**, 257 (1971).
- ²⁹G. Brunton, *Acta Crystallogr. Sect. B* **29**, 2294 (1973).
- ³⁰J. P. Perdew, K. Burke, and M. Ernzerhof, *Phys. Rev. Lett.* **77**, 3865 (1996); **78**, 1396.
- ³¹R. M. Wentzcovitch, Y. Yu, and Z. Wu, *Rev. Mineral. Geochem.* **71**, 59 (2010).
- ³²A. Navrotsky, *Geophys. Res. Lett.* **7**, 709 (1980).
- ³³E. J. Rivera *et al.*, *Astrophys. J.* **634**, 625 (2005).
- ³⁴D. Valencia, R. J. O'Connell, and D. Sasselov, *Icarus* **181**, 545 (2006).
- ³⁵K. Umemoto, R. M. Wentzcovitch, D. J. Weidner, and J. B. Parise, *Geophys. Res. Lett.* **33**, L15304 (2006).
- ³⁶C. D. Martin, W. A. Crichton, H. Liu, V. Prakapenka, J. Chen, and J. B. Parise, *Geophys. Res. Lett.* **33**, L11305 (2006).
- ³⁷T. Tsuchiya and J. Tsuchiya, *Proc. Nat. Acad. Sci. USA* **106**, 1252 (2011).